Journal of Cleaner Production 348 (2022) 131326

Contents lists available at ScienceDirect

Journal of Cleaner Production

journal homepage: www.elsevier.com/locate/jclepro

Climate change-induced variations in blue and green water usage in U.S. urban agriculture

Carolyn M. Cooper [a,1], Jacob P. Troutman [a,b,1], Ripendra Awal [c], Hamideh Habibi [c,2], Ali Fares [c,*]

[a] Department of Civil, Architectural, and Environmental Engineering, The University of Texas at Austin, 301 East Dean Keeton Street, Stop C1700, Austin, TX, 78712, USA
[b] Department of Chemistry, The University of Texas at Austin, 100 East 24th Street, Stop A1590, Austin, TX, 78712, USA
[c] College of Agriculture and Human Sciences, Prairie View A&M University, Prairie View, TX, 77446, USA

ARTICLE INFO

Handling Editor: Kathleen Aviso

Keywords:
Irrigation water requirements
IManSys
Climate change adaptation
Blue water
Green water
Urban agriculture

ABSTRACT

Urban agriculture could assist in meeting the growing global demand for food without overburdening agricultural areas. To fully realize the potential of urban agriculture, it is necessary to better understand the implications of urban agriculture and climate change on the food-energy-water nexus. The objective of this study was to investigate the influence of local climate change on irrigation requirements, and green and blue water usages for turf grass and three common urban agriculture crops (carrots, spinach, and sweet corn) in eight mid-sized U.S. cities. Baseline (1980–2010) and Future (2040–2050) daily climate data were combined with site-specific crop water uptake data to calculate irrigation requirements using the Irrigation Management System Model, IManSys, a numerical simulation model that uses a water balance approach. The irrigation requirements (IRRs) were further used to calculate the energy requirements and associated greenhouse gas emissions for the four crops in each location. Results showed the spatio-temporal impact of climate change on precipitation and evapotranspiration and consequently on crop IRRs. On the east coast, increases in summer precipitation during the crop growing seasons result in relatively small increases in blue water contributions (<222%) to crop water demands. On the west coast, though, decreases in precipitation lead to more drastic increases in blue water contributions (>222%) for these same crops. The energy requirements and greenhouse gas footprints of urban agriculture were weakly correlated to the blue water portion of the IRRs in individual cities but were largely impacted by the source of the water used. Overall, the results highlight the importance of appropriate and thoughtful crop selection for urban agriculture paired with environmentally sustainable water sourcing to maintain, or even reduce, future water and energy footprints of urban agriculture.

1. Introduction

By 2050, the global population is projected to swell to 9.7 billion (United Nations, 2019), with nearly 70% of the population anticipated to live in urban environments. This increase in urban population is expected to result in a *ca.* 171% increase in the global urban footprint as compared to 2015 (Huang et al., 2019; United Nation, 2018). In many regions, urbanization has already led to losses of prime agricultural lands traditionally used for food production and is expected to continue to do so in primarily-agrarian countries (Martellozzo et al., 2015; Seto et al., 2012; Seto and Ramankutty, 2016). The remaining agricultural lands have been facing increasing strain due to intensification (Jiang et al., 2013; Mishra, 2002) and abandonment (Reddy and Reddy, 2007). Ultimately, the trade-off of rural land for urban expansion threatens food security and drives the need for alternative agriculture production systems (Mok et al., 2014).

Urban agriculture could provide an avenue to sustainably address the growing concern of food security in an increasingly urbanized world. Urban agriculture encompasses all stages of producing food and nonfood crops, and livestock directly for an urban market within the local area (Hodgson et al., 2011; Lovell, 2010; Mougeot, 2006). Currently, urban agriculture accounts for approximately 1% of agricultural production but could expand to *ca.* 5–15% through efficient utilization of urban and peri-urban lands (Clinton et al., 2018). The potential production (e.g., biodiversity and nutrient cycling) and non-production (e.g., food justice,

* Corresponding author.
E-mail address: alfares@pvamu.edu (A. Fares).
[1] These authors contributed equally to this work.
[2] Present address: Walter P Moore, 1780 Hughes Landing Boulevard, Suite 450, The Woodlands, Texas 77,380.

https://doi.org/10.1016/j.jclepro.2022.131326
Received 12 October 2021; Received in revised form 19 January 2022; Accepted 10 March 2022
Available online 14 March 2022
0959-6526/© 2022 Published by Elsevier Ltd.

Nomenclature and abbreviations

UA	urban agriculture
IRR	irrigation requirements
GHG	greenhouse gas
IManSys	Irrigation Management System Model
T_{max}	daily maximum temperature (°C)
T_{min}	daily minimum temperature (°C)
ET_O	reference evapotranspiration rate (mm d^{-1} or mm yr^{-1})
ET_C	crop-specific evapotranspiration rate (mm d^{-1} or mm yr^{-1})
K_C	crop coefficient
ΔS	soil column water balance (mm)
P	gross rainfall (mm)
G_w	groundwater contribution to plant water need (mm)
Q_R	surface water runoff (mm)
Q_D	drainage to groundwater (mm)
I	canopy interception (mm)

equity, cultural heritage, and recreation) benefits of urban agriculture have been well-documented in the literature (Alaimo et al., 2008; Draper and Freedman, 2010; Harrison and Winfree, 2015; Kulak et al., 2013; Lovell, 2010; McClintock, 2008; Meenar and Hoover, 2012; Mohareb et al., 2017; Nogeire-McRae et al., 2018; Siegner et al., 2018; Wortman and Lovell, 2013). While some of these benefits (*e.g.*, lessening of embedded energy and greenhouse gas (GHG) emissions in food (Ackerman et al., 2014; Lovell, 2010; Peters et al., 2009), mitigation of urban heat islands (Ackerman et al., 2014; Lin et al., 2015; Lovell, 2010), and aiding in storm water management (Lin et al., 2015)) may help urban climate change mitigation and adaptation efforts, further transdisciplinary studies are necessary to quantify some of the benefits of urban agriculture and its associated technical challenges.

Quantifying and addressing future competition for water resources remain an outstanding challenge for urban agriculture within the food-energy-water nexus (Lin et al., 2015). Globally, climate change is anticipated to exacerbate water scarcity and increase irrigation requirements (IRR) by 2050 (Gosling and Arnell, 2016). Regional climate change variability is anticipated to alter growing seasons and impact the spatio-temporal variability of crops' IRRs (Döll, 2002). Traditionally, many regions rely on municipal water for urban agriculture irrigation, which could stress urban water systems, and the region's water sources (Moglia, 2014; Semananda et al., 2016). Additionally, in the U.S., drinking water standards are higher than those for agricultural irrigation water resulting in excess energy consumption and GHG emission associated with urban agriculture (Dima et al., 2002; Semananda et al., 2016; Ward et al., 2014). Thus, it is necessary to quantify changes in green water availability (*i.e.*, the portion of precipitation used by crops for their evapotranspiration), and the necessary supplemental irrigation water (*i.e.*, blue water which is the crop irrigation water from surface or ground water sources) to understand the longer-term sustainability of urban agriculture.

Several studies have examined and compared regional responses of IRR to potential climate change scenarios for some major growing regions (Awal et al., 2018; Chen et al., 2021; Fares et al., 2016, 2017). Meanwhile, other studies have examined individual regions, *e.g.*, Africa (Jones et al., 2015), southeast Asia (Hong et al., 2016; Mainuddin et al., 2015), the Mediterranean (Saadi et al., 2015; Tanasijevic et al., 2014), western Europe (Díaz et al., 2007), and northern Europe (Riediger et al., 2014). However, all of these analyses have looked at large-scale, conventional agriculture. Few studies have investigated the effects of climate change on IRR of urban agriculture (Lupia et al., 2017). Furthermore, no studies have examined the effect of climate change on green water and blue water contributions for urban agriculture. Yet, if we are to utilize urban agriculture to meet burgeoning population growth and its associated food demands, it is imperative to evaluate urban agriculture in the context of regional climate change which is anticipated to exacerbate water scarcity (Döll, 2009; Gosling and Arnell, 2016; Schewe et al., 2014) and extreme weather events (Attribution of Extreme Weather Events in the Context of Climate Change, 2016; Field et al., 2012; Mal et al., 2008; Stott, 2016).

The overarching goal of this work is to assess the impact of potential climate change scenarios on the spatio-temporal blue and green water needs of some urban farming crops in eight metropolitan areas across the U.S. The specific objectives are: i) to assess future blue and green water requirements and the major water budget components of turf grass, sweet corn, carrots, and spinach in eight mid-size cities using the Irrigation Management System Model (IManSys) water allocation model in tandem with site-specific weather, soil, and crop data and ii) to calculate the concomitant energy requirements and GHG emissions of meeting the estimated irrigation demands.

2. Materials and methods

This analysis investigated the Baseline (1980–2010) and Future (2040–2050) IRR for turf grass and three urban agriculture crops (sweet corn, carrots, and spinach) in eight mid-sized cities across the U.S. The following cities (Fig. 1) were selected to represent the vast spatial climate variability across the United States: Austin, Texas; Buffalo, New York; Jacksonville, Florida; Kansas City, Missouri; Portland, Oregon; Raleigh, North Carolina; Salt Lake City, Utah; and San Jose, California.

2.1. Climate data

Baseline climate data, including daily maximum (T_{max}; °C) and minimum temperatures (T_{min}; °C), precipitation (mm), and solar radiation (MJ/m^2), were obtained from the National Centers for Environmental Prediction Climate Forecast System Reanalysis Global Weather Data for the Soil and Water Assessment Tool ("Global Weather Data for SWAT", 2012). Future climate data, including T_{max}, T_{min}, precipitation ($mm\ s^{-1}$), wind speed ($m\ s^{-1}$), and solar and longwave flux at the surface ($W\ m^{-2}$), were obtained from the International Laboratory for High-Resolution Earth System Prediction (iHESP) for each study site (Chang et al., 2020). The iHESP data set is a 250-year historical and future climate simulation that follows the representative concentration pathway 8.5 (RCP8.5) as prescribed by the Coupled Model Intercomparison Project phase 5 (CMIP5). The model has a 25 km spatial and daily temporal resolution for atmosphere and land surface. A Python script was developed to process and extract the daily climate variables from this published model using the latitude and longitude coordinates of the downtown for each city.

The probability distributions of daily precipitation, T_{max}, and T_{min} were computed for the Baseline and Future data for each study site using Python. The non-parametric Kolmogorov-Smirnov (K–S) two-sample statistical test (Chakravarti et al., 1967; Pratt and Gibbons, 1981) was performed to test the existence of significant differences between the probability distributions of the Baseline and Future climate parameters. Frequency distributions were computed using Python code based on daily climate data time series.

Baseline CO_2 concentrations (ppm) were obtained from the National Oceanic and Atmospheric Administration (NOAA) Global Monitoring Laboratory (Dlugokencky et al, n.d.). The projected CO_2 concentrations were obtained from the Model for the Assessment of Greenhouse Gas Induced Climate Change (Meinshausen et al., 2011) based on the Coupled Model Intercomparison Project 6 (CMIP6) emissions model and the SS5-8.5 scenario.

2.2. Soil hydrologic parameters

Soil hydrologic parameters were extracted from the United States

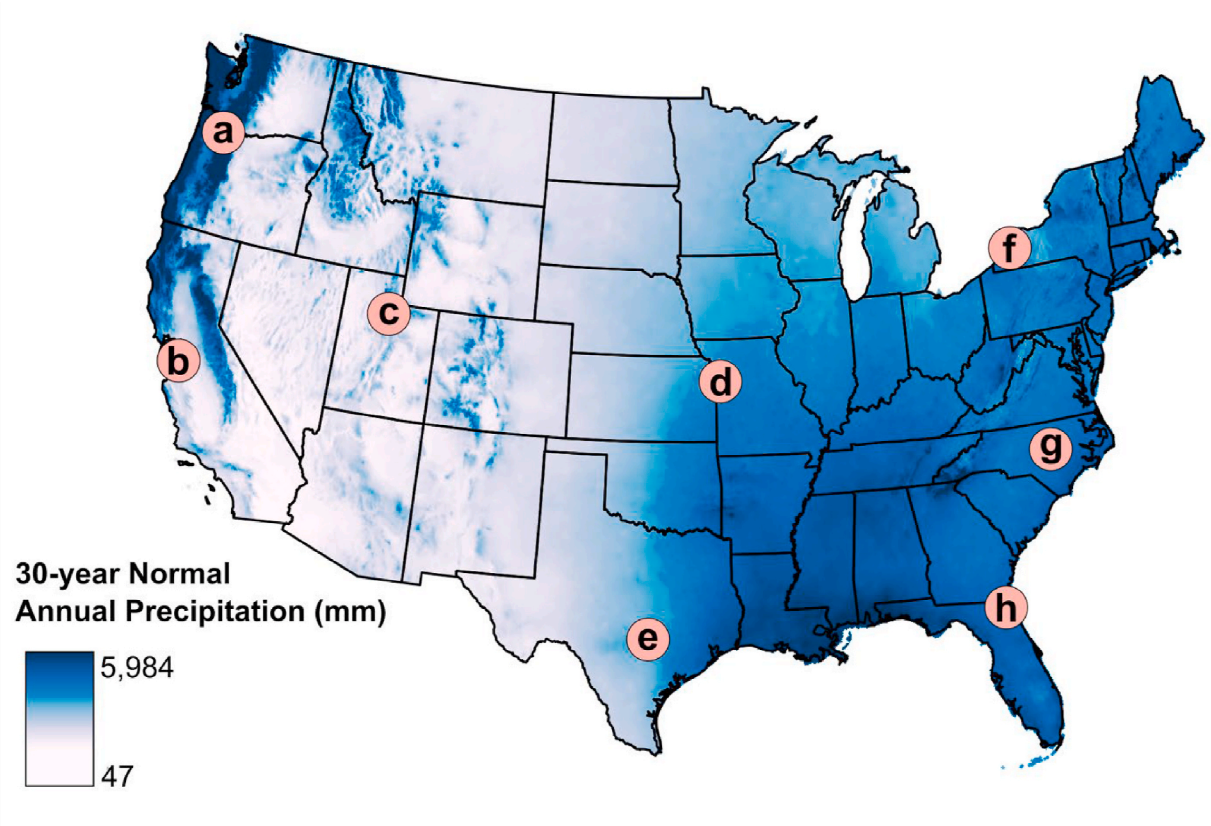

Fig. 1. Map of the United States showing the cities used in the study to represent the different climatic areas: **(a)** Portland, OR, **(b)** San Jose, CA, **(c)** Salt Lake City, UT, **(d)** Kansas City, MO, **(e)** Austin, TX, **(f)** Buffalo, NY, **(g)** Raleigh, NC, and **(h)** Jacksonville, FL. Shaded blue regions represent the average rainfall from 1971 to 2009. Data were collected from the PRISM Climate Group at Oregon State University. (For interpretation of the references to colour in this figure legend, the reader is referred to the Web version of this article.)

Department of Agriculture, Natural Resource Conservation Service, Soil Survey Geographic Database. Simulations were run using the two most common soil types in each county. Table S1 presents a summary of the soil characteristics.

2.3. Crop water uptake parameters

The water budget components for turf grass were used as a reference in each location. Crop water uptake parameters including K_c and the length of the growing season are city-specific and based on previously reported values in the literature ("AgriMet Crop Coefficients: Lawn", 2016, "Turfgrass Crop Coefficients (Kc)", 2021; Aronson et al., 1987; Hill and Barker, 2010; Jia et al., 2009; Pannkuk et al., 2010; Pinnix and Miller, 2019; Romero and Dukes, 2016), while LAI_{max}, root zone depths, and allowable water depletion values were constant across the cities examined (Allen et al., 1998). A summary of the turf grass crop parameters is presented in Table S2.

Sweet corn (*Zea mays* convar. *saccharata* var. *rugosa*), carrots (*Daucus carota* ssp. *sativus*), and spinach (*Spinacia oleracea*) were used in this study. The crop water uptake parameters for these plants (*e.g.*, K_c (Allen et al., 1998), root zone depths (Branham and Deusen, 1986; Brockhoff et al., 2010; Guo et al., 2008; Martinez Hernandez et al., 1991; Murphy et al., 1994; Wu, 1985), maximum leaf area indices (LAI_{max}) (Abazarian et al., 2011; Allen et al., 1998; Hutmacher et al., 1990; Nemadodzi et al., 2017; Williams and Lindquist, 2007), allowable water depletion values (Allen et al., 1998)) and growing seasons were determined from previously reported values found in literature and are summarized in Table S3 **and** S4.

2.4. Energy inputs and greenhouse gas emissions

The energy requirements for the estimated IRRs were calculated using the embedded energy in potable water as reported for each city (Chini and Stillwell, 2018; Eldridge et al., 2010; Mok, 2020; Sowby, 2018; Yonkin et al., 2008). Corresponding GHG emissions were calculated assuming an average CO_2, NO_x, and SO_2 emission for electricity production in each city; these location-specific values were derived from the United States Energy Information Administration for each state ("State Electricity Profiles", 2020). A summary of the energy and GHG intensities can be found in Table S5.

3. Theory

Turf grass, carrots, spinach, and sweet corn IRRs were determined using IManSys (Fares and Fares, 2012). IManSys is a numerical simulation model that combines a water balance approach with crop specific growth parameters, soil hydrologic properties, site-specific weather data, crop- and region-specific growing season, and irrigation system efficiency to calculate crop specific irrigation requirements and major components of the water budget (Awal et al., 2018, 2019; Fares et al., 2016; Khan et al., 2015, 2021). Unlike other water budget models (*e.g.*, the Agricultural Field Scale Irrigation Requirements Simulation), IManSys calculates evapotranspiration (ET_C) for given climate data and accounts for runoff and canopy interception (Fares et al., 2016; Smajstrla and Zazueta, 1988).

The soil water storage capacity is defined as the quantity of water that is available for plant uptake. For a specific soil, the storage capacity is calculated as the equivalent water content between field capacity and plant permanent wilting point multiplied by the depth of plant root

zone. Irrigation is scheduled when a predetermined percentage of the soil water storage capacity is depleted; such point is called the allowable depletion level. The daily water balance of a soil column for a crop-specific root zone (ΔS) can be expressed in terms of equivalent water depth (mm) as follows:

$$\Delta S = P + G_w + IRR_{net} - (Q_D + Q_R + ET_C + I) \quad (1)$$

where P is the gross rainfall (mm), G_w is the contribution of groundwater from the shallow water table (mm), IRR_{net} is the net irrigation requirement (mm), Q_D is the drainage to groundwater (mm), Q_R is the surface water runoff (mm), ET_C is the actual crop evapotranspiration (mm), and I is the canopy rainfall interception (mm). IManSys simulates the water budget of a soil profile depth that is assumed to be equal to the crop root zone depth. The crop root zones are limited by the depth of soil profiles or the water table where applicable. The daily ET_C is the product of the daily reference evapotranspiration rate (ET_O; mm d^{-1}) and K_c (Allen et al., 1998). Daily reference evapotranspiration rates are estimated using the FAO Penman-Monteith equation modified to incorporate future CO_2 emissions and temperature changes as follows (Allen et al., 1998; Fares et al., 2016; Kiziloglu et al., 2009):

$$ET_O = \frac{0.408\Delta(R_n - G) + \gamma \frac{900}{T+273} u_2 (e_s - e_a)}{\Delta + \gamma\left(1 + \frac{r_s}{r_a}\right)} \quad (2)$$

where R_n is the net radiation at the crop surface (MJ m^{-2} d^{-1}), G is the soil heat flux density (MJ m^{-2} d^{-1}), T is the air temperature at a 2 m height above the ground (°C), u_2 is the wind speed at a height of 2 m (m s^{-1}), (e_s−e_a) is the difference between the actual vapor pressure (e_a) and the saturation vapor pressure (e_s) (kPa), Δ is the slope of the saturation vapor pressure curve (kPa °C^{-1}), γ is the psychrometric constant (kPa °C^{-1}), r_s is the bulk surface resistance (s m^{-1}), and r_a is the aerodynamic resistance (s m^{-1}). The ratio r_s/r_a is a function of wind speed at a 2 m height ($0.34u_2$). ET_O can then be translated to ET_c *via* K_c (Allen et al., 1998). The CO_2 concentrations used in this work are 361.7 and 516.5 ppm for Baseline and Future scenarios, respectively.

Irrigation water requirements, or blue water requirements, are calculated as the quantity of water necessary to restore soil water content to field capacity (Fares et al., 2016; Kiziloglu et al., 2009). Assuming negligible groundwater contributions to the root zone (*i.e.*, $G_w = 0$), equation (1) may be transformed to calculate gross IRR (IRR_g) as follows:

$$IRR_g = \frac{IRR_{net}}{\eta} = \frac{ET_C + \Delta S - (P - Q_D - Q_R - I)}{\eta} \quad (3)$$

where η is the efficiency of the irrigation system. All simulations utilized a drip irrigation system with an efficiency of 85%.

Yet, as shown in Equation (3), only a portion of the gross rainfall, known as effective rainfall or green water (P_{eff}), is available to the plant for evapotranspiration. In IManSys, P_{eff} is calculated directly *via* the difference between net rainfall and surface runoff as shown in Equation (3) (Fares and Fares, 2012). The following analysis will consider the fractional contribution of P_{eff} to the water requirements associated with evapotranspiration (χ), which is calculated directly as follows:

$$\chi = \frac{P - I - Q_R - Q_D}{ET_C} = \frac{P_{eff}}{ET_C} \quad (4)$$

Additional details about IManSys can be found in previous publications (Awal et al., 2016, 2018, 2019; Fares et al., 2016, 2017; Fares and Fares, 2012).

4. Results

4.1. Climate characteristics

4.1.1. Annual and monthly trends in climate

Analysis of Baseline precipitation and maximum and minimum temperatures reveals useful trends of these climate variables in the selected cities (Fig. 2a and Table S6). In some cities (*i.e.*, Austin, Buffalo, Raleigh, Kansas City), annual rainfall is relatively uniform across all months. However, the other cities generally have a unimodal rainfall distribution. Jacksonville and Portland have the highest annual rainfall with 1,718 and 1,407 mm y^{-1}, respectively; these annual precipitation exceeded the annual ET_O (1,370 and 943 mm y^{-1}, respectively). However, Portland has a net water deficit (ET_O > precipitation) during five months of the year, compared to only two months of net water deficit in Jacksonville. Salt Lake City and San Jose receive the lowest annual rainfall (575 and 599 mm y^{-1}, respectively), and in both cities annual ET_O is *ca.* twice the annual rainfall (1,056 and 1,294 mm y^{-1}, respectively). Overall, annual ET_O is highest in the city of Austin (1,507 mm y^{-1}) and lowest in Buffalo (906 mm y^{-1}); annual ET_O exceeded annual precipitation in half of the cities, which leads to a deficit in soil moisture available for the plants and irrigation is required to address the crop water needs (Table S6). These results agree with previous work demonstrating the importance of ET_O in the hydrologic cycle (Liu et al., 2010).

As anticipated, the estimated Future climate data (2040–2050) show increased T_{max}, T_{min}, and ET_O across all eight cities (Fig. 2a and Table S7). Moreover, the distributions of precipitation, ET_O, T_{max}, and T_{min} during the Future scenario are statistically different from those during the Baseline period (Figs. S2–S5). In agreement with the Baseline data, Jacksonville is projected to continue having the highest annual rainfall (2,247 mm y^{-1}) among the cities in this study; however, Raleigh will replace Portland as the city with the second highest annual rainfall (1,598 mm y^{-1}). In both cities, annual rainfalls are expected to exceed annual ET_O (1,969 and 1,587 mm y^{-1}, respectively). In the Future, the rainfall distribution in Jacksonville is predicted to change; there will be four months with a net water deficit compared to only two during the Baseline period. Raleigh is predicted to experience seven months of net water deficit, compared to six in the Baseline period. Salt Lake City and San Jose are projected to maintain their rankings and will receive the least rainfall (736 and 650 mm y^{-1}, respectively) with each city experiencing net water deficit for nine months of the year. The magnitude of the annual deficits is projected to increase for both cities in the Future scenario versus the Baseline period. Salt Lake City's future annual ET_O is 2,212 mm y^{-1}, which is three-times larger than its rainfall; San Jose's annual ET_O (2,818 mm y^{-1}) is four-times greater than its rainfall.

As expected, increases in T_{max} and T_{min} result in elevated ET_O across all eight cities. Future annual ET_O is anticipated to be highest in San Jose and Austin (2,818 and 2,577 mm y^{-1}, respectively) and lowest in Buffalo and Raleigh (1,321 and 1,587 mm y^{-1}). Six of the eight cities (San Jose, Salt Lake City, Buffalo, Portland, Kansas City, and Austin) are expected to experience net annual water deficit, with annual soil water deficits ranging between −126 mm y^{-1} (Buffalo) and −2,168 mm y^{-1} (San Jose). Additionally, two cities are anticipated to experience monthly deficits greater than 350 mm y^{-1}: Portland in July and San Jose during the June–August period.

4.1.2. Seasonal trends in climate

While monthly and annual trends give a clear description of the climate's variability with location, it can be difficult to correlate these trends with agricultural water budgets due to the seasonality of various crops. As such, seasonal analyses were adopted for each location to examine the effect of Baseline and Future climate scenarios on the four crops (Fig. 2b and Table S8). Seasons were defined as winter (December, January, February), spring (March, April, May), summer (June, July, August), and autumn (September, October, November). The data show

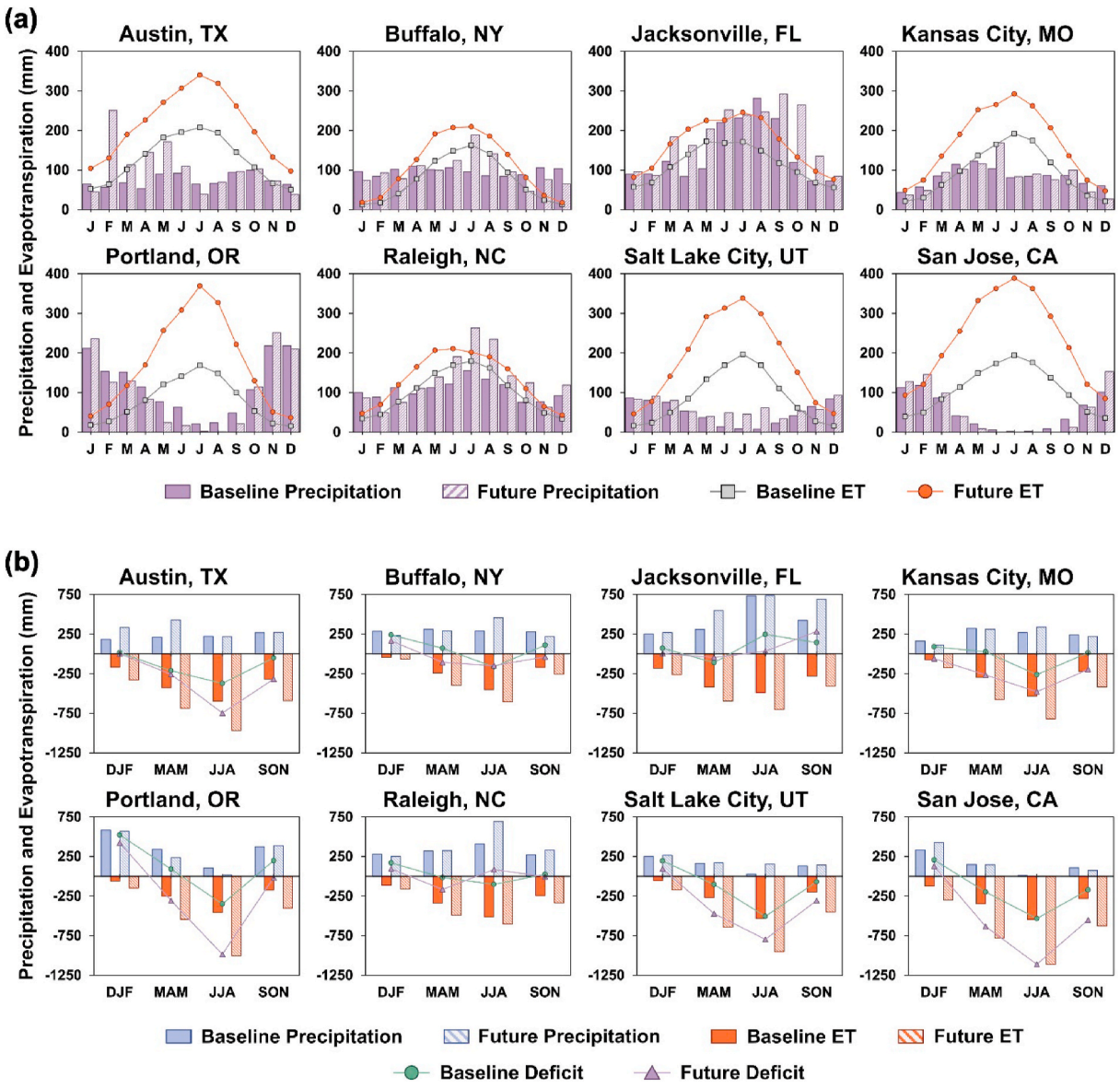

Fig. 2. **(a)** Baseline (1980–2010) and Future (2040–2050) monthly climate characteristics of the eight cities: Baseline precipitation (solid purple bars), Future precipitation (striped purple bars), Baseline ET_O (grey squares), and Future ET_O (red circles). **(b)** Baseline (1980–2010) and Future (2040–2050) seasonal climate characteristics of the eight studied cities: Baseline precipitation (solid blue bars), Future precipitation (striped blue bars), Baseline ET_O (solid orange bars), Future ET_O (striped orange bars), Baseline deficit (green circles), and Future deficit (purple triangles). The seasons are defined as winter (DJF), spring (MAM), summer (JJA), and autumn (SON). (For interpretation of the references to colour in this figure legend, the reader is referred to the Web version of this article.)

the seasonality of the rainfall where one or two seasons generally dominate the annual precipitation and ET_O totals in most of the cities. For example, during the Baseline period in San Jose, the summer months account for *ca.* 42% of the yearly ET_O, while nearly 55% of the annual rainfall occurs during the winter months. In general, values of both Baseline and Future ET_O are highest during the summer months. For cities located in the east (Buffalo, Jacksonville, and Raleigh), both Baseline and Future precipitations are highest in the summer; for cities in the west (Portland, Salt Lake City, and San Jose), Baseline and Future precipitations are highest during the winter. Both Austin and Kansas City experience a relatively uniform distribution of precipitation amongst the seasons.

As stated above, the difference between rainfall and ET_O directly determines the soil water deficit. For cities that receive mostly winter rainfall, the most consequential deficits occur during the summer. San Jose and Salt Lake City experience the greatest Baseline summer deficits (−533 and −505 mm, respectively), while Raleigh and Buffalo experience the smallest Baseline summer deficits (−100 and −164 mm, respectively). In contrast to the other cities, Jacksonville experiences a water surplus during the summer (245 mm). In the Future, San Jose and Portland experience the most substantial summer deficits (−1,112 and −985 mm, respectively), while Buffalo experiences the smallest deficit (−147 mm). In the Future, both Jacksonville and Raleigh are projected to experience a water surplus during the summer (34 and 87 mm, respectively).

4.2. *Effect of soil on water budget components*

For each city, water budget components were calculated using the two most common soil complexes in the corresponding county to best represent the chosen location (Table S1). Statistical analyses *via* K–S two-sample tests, F-tests for sample variances, and t-tests of the turf grass IRR for each location did not indicate significant differences between the soil complexes (Table S9). This was further confirmed by

comparing standard errors of turf grass IRR within each city (Fig. S6). However, it should be noted that this comparison is limited by the minimal variation in soil type at the county level. As such, the water budgets presented in subsequent sections represent averages of the two main soil complexes in each location.

4.3. Irrigation requirements for turf grass

Analysis of the Baseline and Future IRR for turf grass highlights the relationships between precipitation, ET_C, soil water deficit, and IRR (Fig. 3 and Table S10). The turf grass IRR during the Baseline period are highest in cities west of the Rocky Mountains (San Jose, Salt Lake City, and Portland). The high IRR for San Jose and Salt Lake City (856 and 488 mm, respectively) are consistent with the large annual water deficits experienced by both locations. However, Portland has the third highest turf grass IRR (501 mm), despite receiving the second highest annual rainfall and having the largest annual water surplus. In this instance, drainage accounts for *ca.* 56% of the water loss and thus has a large impact on IRR (Fig. S7). Additionally, most of the irrigation is needed during the summer, but most precipitation falls during the winter. Thus, the percentage of green water contributions to the water requirements for evapotranspiration (χ) are the lowest in San Jose, Salt Lake City, and Portland (20%, 34%, and 42%, respectively).

The turf grass IRRs are lowest during the Baseline period in Kansas City (262 mm), Buffalo (156 mm), and Raleigh (148 mm). The low IRR for Kansas City is consistent with the seasonal climate; the location experiences small ($\leq$90 mm) water surpluses during the winter, spring, and autumn and a moderate deficit (−262 mm) during the summer. In Buffalo, turf grass is active during a short period of time in the summer and early autumn months, in comparison with the other locations, during which there is a relatively low water deficit of −164 mm and a surplus of 109 mm. As such, 78% of the turf grass water requirements are met from green water. Similarly, Raleigh experiences small deficits during spring and summer (−16 and −100 mm, respectively) and an excess (27 mm) during autumn, corresponding to the local turf grass season. Thus, green water fulfills 81% of the turf grass water requirements.

Future turf grass IRRs reveal regional trends in ET_C, precipitation, and soil water deficits caused by climate change variability. Generally, seasonal water deficits increase as we move from the east to the west of the contiguous U.S. Cities east of the Mississippi River are anticipated to experience substantial net water surpluses (>500 mm). In contrast, cities west of the Rocky Mountains are predicted to witness net water deficits (>288 mm). As in the Baseline period, San Jose has the highest IRR (2,041 mm), but Portland has the second highest IRR (1,420 mm). Ultimately, Portland and San Jose experience the largest fractional increases in IRR (183% and 139%, respectively). Furthermore, only 10 and 20%, respectively, of turf grass requirements are from green water for San Jose and Portland. Portland has the largest decrease in the contribution of green water to meeting its turf grass water requirements. Raleigh has the lowest IRR (80 mm) in the Future scenario, and green water meets 92% of the turf grass water requirements. Buffalo is anticipated to still have the second lowest required IRR (210 mm). Similarly, while green water contributions decrease slightly, 74% of Buffalo's turf grass water requirements are anticipated to come from green water. Jacksonville is expected to have 78% of its turf grass water requirements supplied from green water in the Future period, surpassing Buffalo. Ultimately, Jacksonville and Buffalo are anticipated to see the smallest increases in IRR (7% and 34%, respectively). Interestingly, Raleigh is anticipated to see a decrease in turf grass IRR of *ca.* 46%, which is unique among the studied cities.

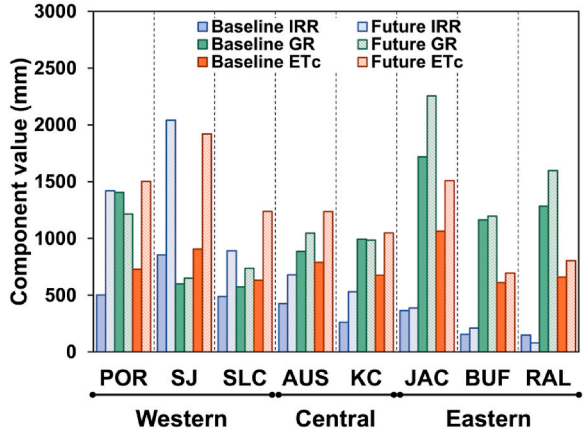

Fig. 3. Baseline (solid) and Future (striped) water budget components for turf grass in each of the eight cities: Baseline IRR (solid blue), Future IRR (striped blue), Baseline gross rainfall (solid green), Future gross rainfall (striped green), Baseline ET_c (solid orange), and Future ET_c (striped orange). The Western region, defined as west of the Rocky Mountains, includes Portland, OR (POR), San Jose, CA (SJ), and Salt Lake City, UT (SLC). The Central region, between the Mississippi River and the Rocky Mountains, includes Austin, TX (AUS) and Kansas City, MO (KC). The Eastern region, defined as east of the Mississippi River, includes Jacksonville, FL (JAC), Buffalo, NY (BUF), and Raleigh, NC (RAL). (For interpretation of the references to colour in this figure legend, the reader is referred to the Web version of this article.)

4.4. Irrigation requirements for urban agriculture

The water budget components of sweet corn, carrots, and spinach were calculated for the eight locations using Baseline and Future climate data to assess the impacts of climate change on urban agriculture. Broadly, climate change is anticipated to increase blue water demands of urban agriculture food crops in the U.S. (Fig. 4). As a result, Future IRR increased in 23 of the 24 scenarios studied; IRR increased by 50–100% in nine scenarios, 100–200% in seven scenarios, and more than 200% in three scenarios. A summary of water budget response to climate change is shown in Figs. S8–S10 and by Tables S11–S13.

4.4.1. Sweet corn

Baseline trends in sweet corn IRR are like those observed in turf grass (Fig. 4a). Salt Lake City and San Jose currently have the highest calculated sweet corn IRR (496 and 377 mm, respectively), the highest in-season water deficits (−461 and −491 mm, respectively), and the lowest green water contributions to crop water requirements (1 and 6%, respectively). These results agree with the previously described climate characteristics of the Western U.S., where below average precipitation coupled with near-average ET_C produce the largest soil water deficits and increase demand for blue water. As seen by the seasonal climate distributions, sweet corn grown in western cities will need to rely almost completely on blue water, which increases the demand of fresh water. In contrast, Raleigh and Jacksonville currently experience the lowest water deficits (−104 and −99 mm, respectively) during the growing season due to relatively high precipitation and near average ET_C compared to the other cities examined. Consequently, Raleigh and Jacksonville have the lowest need for irrigation from blue water (115 and 145 mm, respectively). As with turf grass, sweet corn in Raleigh, Buffalo, and Jacksonville meets about half of its water needs (58, 51, and 48%, respectively) from green water. These results concur with the previously described climate characteristics described in the Eastern U.S.

Sweet corn dependence on blue water is projected to increase in the Future period in seven of the eight cities. However, the relative increases in blue water for irrigation are not consistent, ranging from 18 to 274%. San Jose (978 mm) is projected to displace Salt Lake City as the city with the highest blue water needs. Portland is projected to witness the largest relative increase in blue water needs and experience the second-highest IRR (911 mm). These dynamics are congruous with Portland's anticipated increase in T_{max} (>10 °C), which significantly raises ET_C, coupled with a substantial decrease in precipitation during the growing season

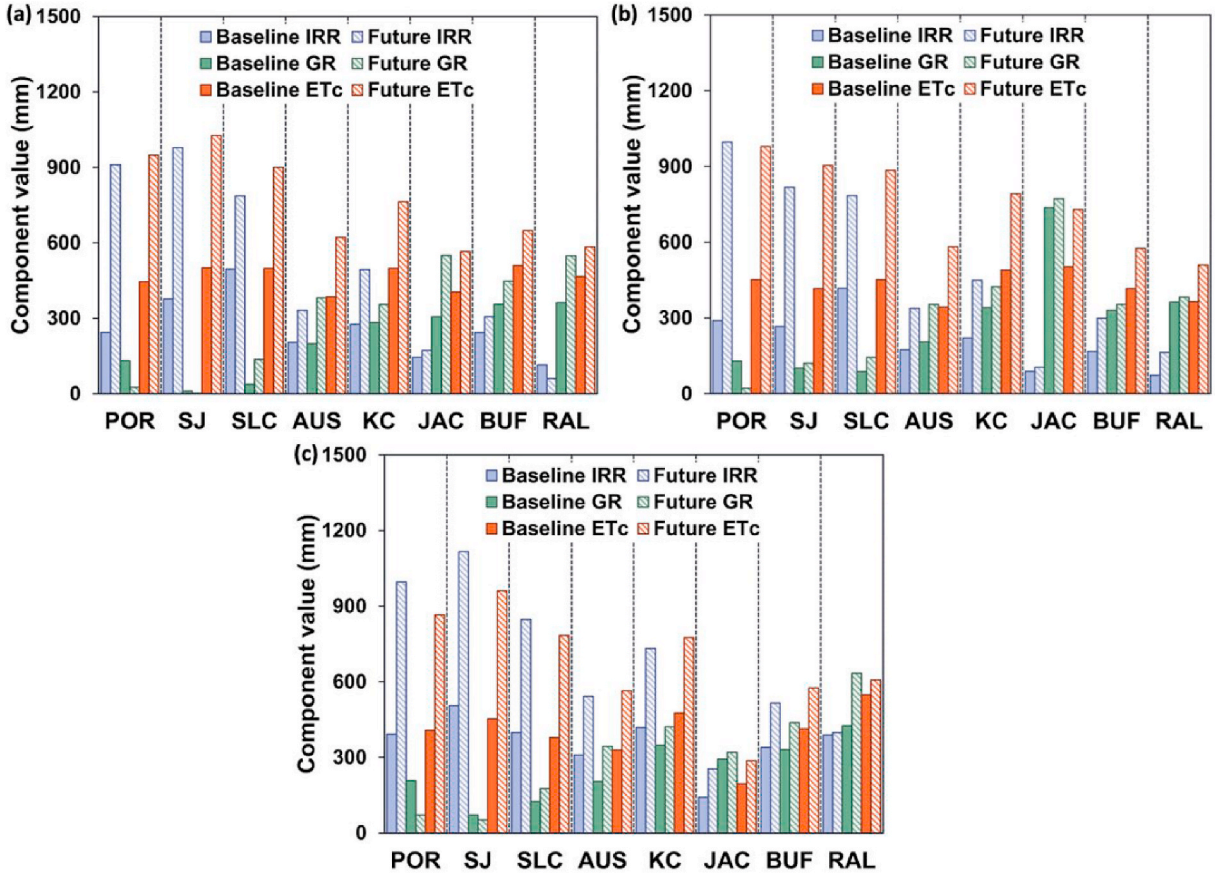

Fig. 4. Baseline (solid bars) and Future (striped bars) irrigation requirements (blue), gross rainfall (green), and ETc (orange) for **(a)** sweet corn, **(b)** carrots, and **(c)** spinach. (For interpretation of the references to colour in this figure legend, the reader is referred to the Web version of this article.)

(from 131 to 26 mm). Thus, Portland experiences a 91% decrease in the fractional contributions of green water to the sweet corn water requirements. In agreement with the Baseline data, sweet corn grown in Raleigh will continue to have the smallest blue water footprint, as it leads the other cities by having the lowest IRR (61 mm), because of the combined effect of a significant increase (51%) in precipitation and a small increase (25%) in ET_C. As such, 79% of the sweet corn irrigation water is green water. Furthermore, as with turf grass, Raleigh is the only city that is projected to experience an increase in the contribution of green water and, thus, a 47% decrease in its sweet corn IRR.

4.4.2. Carrots

Regional trends in climate also strongly influence Baseline and Future carrot IRR (Fig. 4b). Carrots grown in cities west of the Rocky Mountains have the highest dependence on blue water to meet water requirements in both the Baseline and Future scenarios; carrots grown in cities east of the Mississippi River require the smallest amounts of blue water during both the Baseline and the Future period. All cities examined in the study are projected to experience an increase in carrots' IRR during the Future period in comparison with the Baseline.

Salt Lake City, Portland, and San Jose have the highest Baseline IRR for carrots (417, 286, and 267 mm, respectively). These three cities are also estimated to have the highest Future IRR for carrots (802, 994, and 817 mm, respectively). In addition, Portland and San Jose are expected to have the largest increase in IRR (247 and 206%, relatively). As anticipated, green water contributions to carrot water needs are the lowest in Salt Lake City, Portland, and San Jose during both the Baseline and Future periods.

In contrast, Raleigh and Jacksonville have the lowest Baseline IRR for carrots (73 and 89 mm, respectively). This order is projected to switch during the Future scenario, with Jacksonville having a smaller blue water requirement than Raleigh (105 versus 163 mm, respectively). Carrots grown in Jacksonville and Raleigh meet the largest portion of their water requirements from green water compared to the other cities in this study; this trend is true in both the Baseline period and the Future period. The dynamics at play in the relationship between Baseline and Future precipitation, green water, evapotranspiration, and blue water in the Western and Eastern U.S. were detailed in the previous section.

4.4.3. Spinach

Baseline trends in spinach IRR deviate from the broad regional trends observed for sweet corn and carrots (Fig. 4c). Jacksonville has the lowest Baseline IRR (142 mm), which is at least less than half of the IRRs for the spinach grown in the other cities (≥310 mm). This result is consistent with the prevailing weather conditions during the spinach growing season. Jacksonville is the only city to experience a water surplus during the growing season (98 mm); as such, 50% of the spinach water requirements are met from green water. However, it should be noted that the spinach growing season in Jacksonville runs from December through early March, significantly earlier than that of either sweet corn or carrots. It is also significantly earlier than the spinach growing season in every city but Austin, where the spinach season is early February through mid-May. San Jose and Kansas City have the highest spinach IRR during the Baseline period (505 and 414 mm, respectively). San Jose receives the lowest precipitation but has the third highest ET_C, resulting in the greatest seasonal water deficit (−381 mm). Interestingly, while the seasonal deficit in Kansas City is the fourth largest (−128 mm), close examination of the monthly ET_C and precipitation reveals soil moisture surplus at the start of the season (14 mm) to a substantial deficit in the final month (−95 mm). Thus, the poor precipitation distribution across

the growing season in Kansas City contributes to large amount of blue water needed by carrots.

All the cities examined are projected to experience an increase in IRR under the Future period in comparison to the Baseline. Furthermore, seven of the eight cities examined experience a decrease in the contributions of green water to the overall IRR. Previously discussed regional trends in climate dominate the change from Baseline to Future requirements, as cities within the Eastern U.S. are forecast to benefit from green water to meet spinach water needs resulting in the lowest IRR. However, spinach grown in the Western U.S. continue to depend primarily on blue water to meet its water requirements; as such, these cities are expected to have the highest IRR. This trend matches the trend in Future seasonal water deficits. Spinach grown in Jacksonville and Raleigh will meet 34% and 51% of its water requirements with green water; consequently, these cities have the lowest estimated spinach IRR for the Future period (253 and 399 mm, respectively). San Jose and Portland are anticipated to have the highest Future IRR (1,117 and 990 mm, respectively), the largest relative increases in IRR (121% and 156%, respectively), and the lowest green water contributions to their water requirements for evapotranspiration requirements (3% and 5%, respectively). These results are consistent with the doubling of ET_C paired with a decrease in precipitation during the growing season.

In cities with substantial increases in IRR requirements, growing season selection and optimization may play an increasingly important role. For example, utilization of a spinach growing season from September to November instead of April to July in Portland reduces the Baseline IRR from 387 mm to 62 mm. The difference in the seasons is even more evident in the Future. While the ET_c more than doubles in both seasons, the winter season experiences a slight increase in precipitation while the summer seasons experiences a substantial decrease in precipitation. Ultimately, these seasonal differences result in a considerable difference in IRR, and green water, between the winter and summer seasons (199 mm and 990 mm, respectively). While this example solely highlights a single crop in a single city, it is likely that similar opportunities for crop and season optimization exist in other cities.

4.5. Urban agriculture energy and greenhouse gas emissions

The energy and GHG footprint of urban agriculture are weakly related to its efficiency in using green water and on its ability to decrease its dependence on blue water (Fig. 5 and Fig. S11). Crops grown in San Jose have the highest energy footprint per acre during the Baseline and Future periods for all studied agriculture crops examined due to their elevated IRR demand. In contrast, crops grown in Buffalo have a relatively low dependence on blue water. Buffalo's potable water also has a low energy requirement (*ca.* 580 kWh per million gallons of water) as compared to the other cities of the study (Yonkin et al., 2008). Thus, carrots and spinach grown in Buffalo have the lowest energy footprint and sweet corn has the second-lowest energy footprint. Interestingly, Portland has the lowest energy footprint for sweet corn and the second-lowest energy footprint for carrots and spinach, despite having relatively high dependence on blue water. This is primarily due to the low energy requirement of Portland's potable water (*ca.* 490 kWh per million gallons of water) (Chini and Stillwell, 2018). However, sweet corn grown in Raleigh has the lowest Future energy footprint mainly due to its low need for blue water despite the relatively high energy requirement of the city's potable water (*ca.* 2060 kWh per million gallons of water).

The greenhouse gas footprint of urban agriculture as expressed by CO_2, NO_x, and SO_2 emissions follows relatively similar trends as the energy (Fig. S11). As with the energy usage, Buffalo and Portland are estimated to currently have to lowest CO_2 emissions per acre, and Buffalo is projected to have the lowest CO_2 emission under the Future scenario. Thus, while we may broadly anticipate increases in the energy use and greenhouse gas emissions of urban agriculture as IRR increases, a clean energy source with a low greenhouse gas footprint could mitigate that effect.

5. Discussion

Climate change is anticipated to have a spatio-temporal variable impact on precipitation and evapotranspiration. These spatially specific temporal changes are shown to play a major role in changes in future IRR, and green and blue water usage. An illustration of such changes is shown through comparing the projected IRR increases in Portland to those of Raleigh. While Portland is projected to experience IRR increases of more than 150% for turf grass and the other crops examined, Raleigh is projected to enjoy decreases in IRR for both turf grass and sweet corn.

Further, results demonstrated that temporal changes in precipitation and evapotranspiration are expected to have a spatially variable impact on the water requirements and water sources (e.g., green water vs. blue water) across the contiguous U.S. As expected, the results highlight the importance of spatial variability; cities in the Eastern U.S. are anticipated to experience increases in precipitation that result in relatively small changes in soil water deficits. In contrast, cities in the Western U.S. are anticipated to see a substantial increase in soil water deficits during the growing season. These climactic trends drive smaller changes in IRR in the Eastern U.S. than in the Western U.S. In particular, Raleigh is the only city that experiences a decrease in IRR between the Baseline and Future periods and consistently has one of the lowest blue water contributions. However, its municipal water has relatively high energy and carbon footprint resulting in Raleigh not having the lowest energy intensity and GHG footprint. Thus, appropriate climate change adaptation strategies for urban agriculture may vary regionally.

One such strategy could be changing the crop's growing seasons.

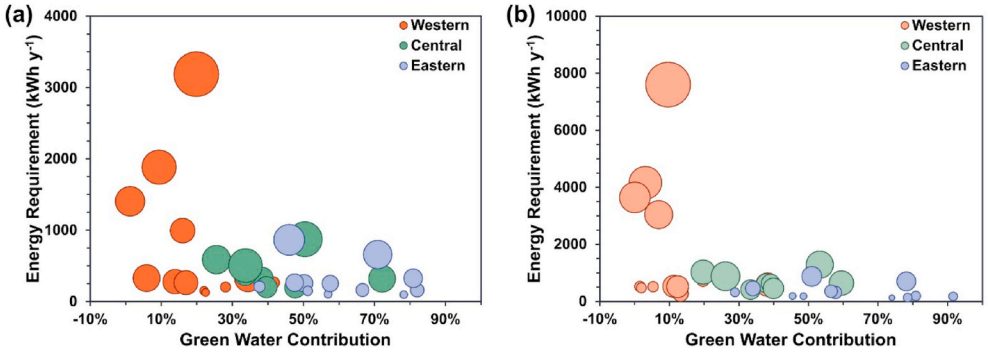

Fig. 5. (a) Baseline and **(b)** Future relationships between the percent of crop water needs met by green water, the required energy input, and the resultant CO_2 emissions (represented as the circle diameter) to meet the urban agriculture IRRs in the Western (orange), Central (green), and Eastern (blue) U.S. Calculated Pearson correlation coefficients are **(a)** $r = -0.392$, and **(b)** $r = -0.434$.

Modifying the growing seasons of crops in cities where such changes are possible could maximize and minimize green water and blue water usages, respectively. Because less irrigation water is required, the energy and resulting GHG emissions will also be lower. For example, altering the spinach growing season from summer to winter in Raleigh and Portland reduces the Future irrigation requirements 43% and 80%, respectively. Similarly, altering the carrot growing season from summer to winter in Raleigh reduces the Future irrigation requirements by 51%. Furthermore, careful consideration of crop choice may help in mitigating the irrigation water demand of urban agriculture. Yet, additional work would be necessary to identify appropriate crops, seasonal adjustments, and other potential approaches to minimize the future water demand of urban agriculture.

Finally, in considering urban agriculture within the food-energy-water nexus, it is important to acknowledge the role of the embedded energy in potable water and the GHG footprint of the electric grid itself. While the GHG footprint of urban agriculture crops broadly follow trends in blue water usage and its corresponding energy needs, cities with either elevated reported embedded energy (e.g., Raleigh, San Jose) or energy sources with a high GHG footprint (e.g., Kansas City, Salt Lake City) often have relatively high GHG footprints. This effect is particularly evident for San Jose, where large increases in IRRs are paired with both high energy requirements of water and a high GHG intensity of electricity (Fig. S11). Thus, in addition to optimizing the water requirements of urban agriculture, reducing the energy intensity of municipal water, expanding the utilization of alternative, lower energy intensity water sources (e.g., rainwater, storm water runoff, grey- or blackwater), and/or incorporating renewable energy sources could enable urban agriculture with a lower GHG footprint.

6. Conclusions

As we look to the future, it is evident that increasing population and climate change will require careful consideration to feed the 10 billion while mitigating the water and energy footprint of agriculture. Urban agriculture may play a role within a diverse set of solutions in meeting this need. Additionally, it is first necessary to understand how climate change may impact the future localized water and energy requirements for urban agriculture. As such, we cannot currently make specific recommendations to urban farmers due to the number of factors that govern agriculture not explored in this work. For example, this study examines a limited number of crops under one crop husbandry practice in only few cities, all located in the contiguous United States. However, this study serves as an important first step in understanding how major influences, like climate change, will impact future urban agriculture.

This study illustrates the concept of how regional variability of climate change impacts ET_O and precipitation. Climate change is anticipated to create a statistically significant difference between the distributions of precipitation, ET_O, T_{max}, and T_{min} of the Future and Baseline period. Furthermore, one or two seasons generally dominate precipitation and ET_O in most cities examined. The frequently unimodal behavior impacts the interplay between green water and blue water requirements when the growing seasons for urban agriculture crops falls outside of these seasons.

These climactic changes are reflected in the results for both turf grass and urban agriculture crops. In seven of the eight cities, turf grass IRR increased due to an increase in soil water deficits from poorly paired changes in ET_O and precipitation. Changes in green and blue water utilization by turf grass begin to indicate the potential for either turf grass or urban agriculture to strain municipal water resources. As with turf grass, changes in IRR, green water, and blue water vary both spatially and temporally. Future IRR, energy, and GHG footprints increased in 23 of 24 scenarios examined. Furthermore, in 19 of 24 scenarios, the relative blue water usage increased. Yet, the magnitude of blue water increase varied widely. These results ultimately highlight the importance of localized consideration of crop selection for urban agriculture to maintain or reduce the future water and energy footprint of urban agriculture. Additionally, similar studies in other countries experiencing large population migrations to urban areas may prove extremely useful in understanding how climate change will impact the food availability in these nations.

Funding

Funding for this work was provided by the National Science Foundation under Grant No. DGE-1828974 and the U.S. Department of Agriculture National Institute of Food and Agriculture Evans-Allen Project 1021753.

CRediT authorship contribution statement

Carolyn M. Cooper: Conceptualization, Investigation, Writing – original draft, Writing – review & editing, Visualization. **Jacob P. Troutman:** Conceptualization, Formal analysis, Investigation, Writing – original draft, Writing – review & editing, Visualization. **Ripendra Awal:** Conceptualization, Methodology, Writing – review & editing. **Hamideh Habibi:** Data curation. **Ali Fares:** Conceptualization, Methodology, Writing – review & editing, Supervision.

Declaration of competing interest

The authors declare that they have no known competing financial interests or personal relationships that could have appeared to influence the work reported in this paper.

Acknowledgement

The authors thank Dr. Charles Werth, Laura Klopfenstein, and the Innovation at the Nexus of Food-Energy-Water Systems Scholars Program at the University of Texas at Austin. The authors also thank Dr. Ping Chang and Dr. Abishek Gopal of the International Laboratory for High-Resolution Earth System Prediction (iHESP) at Texas A&M University who provided climate data used for the Future scenario. The authors also thank Dr. Atikur Rahman for reviewing the article and providing feedback.

Appendix A. Supplementary data

Supplementary data to this article can be found online at https://doi.org/10.1016/j.jclepro.2022.131326.

References

Abazarian, R., Azizi, M., Shoor, M., Arvin, P., 2011. Effects of foliar application of zinc on physiological indices and yield of three spinach cultivars in Bojnourd , Iran. Afr. J. Agric. Res. 6, 6572–6574. https://doi.org/10.5897/AJAR11.477.

Ackerman, K., Conard, M., Culligan, P., Plunz, R., Sutto, M.P., Whittinghill, L., 2014. Sustainable food systems for future cities: the potential of urban agriculture. Econ. Soc. Rev. 45, 189–206.

AgriMet Crop Coefficients: Lawn, 2016 [WWW Document], URL. https://www.usbr.gov/pn/agrimet/cropcurves/LAWNcc.html, 9.8.20.

Alaimo, K., Packnett, E., Miles, R.A., Kruger, D.J., 2008. Fruit and vegetable intake among urban community gardeners. J. Nutr. Educ. Behav. 40, 94–101. https://doi.org/10.1016/j.jneb.2006.12.003.

Allen, R.G., Pereira, L.S., Raes, D., Smith, M., 1998. Crop Evapotranspiration - Guidelines for Computing Crop Water Requirements - FAO Irrigation and Drainage Paper 56. FAO - Food and Agriculture Organization of the United Nations, Rome.

Aronson, L.J., Gold, A.J., Hull, R.J., Cisar, J.L., 1987. Evapotranspiration of cool-season Turfgrasses in the Humid Northeast 1. Agron. J. 79, 901–905. https://doi.org/10.2134/agronj1987.00021962007900050029x.

Attribution of Extreme Weather Events in the Context of Climate Change, 2016. The National Academies Press, Washington, D.C. https://doi.org/10.17226/21852.

Awal, R., Bayabil, H.K., Fares, A., 2016. Analysis of potential future climate and climate extremes in the brazos headwaters Basin. Texas. Water 8, 1–18. https://doi.org/10.3390/w8120603.

Awal, R., Fares, A., Bayabil, H., 2018. Assessing potential climate change impacts on irrigation requirements of major crops in the brazos headwaters Basin. Texas. Water 10. https://doi.org/10.3390/w10111610.

Awal, R., Fares, A., Habibi, H., 2019. Optimum turf grass irrigation requirements and corresponding water- energy-CO2 Nexus across Harris County, Texas. Sustainability 11, 1–12. https://doi.org/10.3390/su11051440.
Branham, B.E., Deusen, J. Van, 1986. Examining the Turfgrass Rootzone with Minirhizotrons, 2. Agronomy abstracts.
Brockhoff, S.R., Christians, N.E., Killorn, R.J., Horton, R., Davis, D.D., 2010. Physical and mineral-nutrition properties of sand-based turfgrass root zones amended with biochar. Agron. J. 102, 1627–1631. https://doi.org/10.2134/agronj2010.0188.
Chakravarti, I.M., Laha, R.G., Roy, J., 1967. Handbook of Methods of Applied Statistics. In: Techniques of Computation of Descriptive Methods, and Statistical Inference, 1. John Wiley, New York, NY.
Chang, P., Zhang, S., Danabasoglu, G., Yeager, S.G., Fu, H., Wang, H., Castruccio, F.S., Chen, Y., Edwards, J., Fu, D., Jia, Y., Laurindo, L.C., Liu, X., Rosenbloom, N., Small, R.J., Xu, G., Zeng, Y., Zhang, Q., Bacmeister, J., Bailey, D.A., Duan, X., DuVivier, A.K., Li, D., Li, Y., Neale, R., Stössel, A., Wang, L., Zhuang, Y., Baker, A., Bates, S., Dennis, J., Diao, X., Gan, B., Gopal, A., Jia, D., Jing, Z., Ma, X., Saravanan, R., Strand, W.G., Tao, J., Yang, H., Wang, X., Wei, Z., Wu, L., 2020. An unprecedented set of high-resolution Earth system simulations for understanding multiscale interactions in climate variability and change. J. Adv. Model. Earth Syst. 12 https://doi.org/10.1029/2020MS002298.
Chen, Y., Marek, G.W., Marek, T.H., Porter, D.O., Brauer, D.K., Srinivasan, R., 2021. Modeling climate change impacts on blue, green, and grey water footprints and crop yields in the Texas High Plains, USA. Agric. For. Meteorol. 310, 108649. https://doi.org/10.1016/j.agrformet.2021.108649.
Chini, C.M., Stillwell, A.S., 2018. The state of U.S. Urban water: data and the energy-water nexus. Water Resour. Res. 54, 1796–1811. https://doi.org/10.1002/2017WR022265.
Clinton, N., Stuhlmacher, M., Miles, A., Uludere Aragon, N., Wagner, M., Georgescu, M., Herwig, C., Gong, P., 2018. A global geospatial ecosystem services estimate of urban agriculture. Earth's Future 6, 40–60. https://doi.org/10.1002/2017EF000536.
Díaz, J.A.R., Weatherhead, E.K., Knox, J.W., Camacho, E., 2007. Climate change impacts on irrigation water requirements in the Guadalquivir river basin in Spain. Reg. Environ. Change 7, 149–159. https://doi.org/10.1007/s10113-007-0035-3.
Dima, S.J., Ogunmokun, A.A., Nantanga, T., 2002. The Status of Urban and Peri-Urban Agriculture: Windhoek and Oshakati, Namibia. Windhoek, Namibia.
Dlugokencky, E., Tans, P.. Trends in atmospheric carbon dioxide. n.d., [WWW Document]. URL. https://gml.noaa.gov/ccgg/trends/g_data.html, 8.9.20.
Döll, P., 2002. Impact of climate change and variability on irrigation requirements: a global perspective. Climatic Change 54, 269–293. https://doi.org/10.1023/A:1016124032231.
Döll, P., 2009. Vulnerability to the impact of climate change on renewable groundwater resources: a global-scale assessment. Environ. Res. Lett. 4, 035006 https://doi.org/10.1088/1748-9326/4/3/035006.
Draper, C., Freedman, D., 2010. Review and analysis of the benefits, purposes, and motivations associated with community gardening in the United States. J. Community Pract. 18, 458–492. https://doi.org/10.1080/10705422.2010.519682.
Eldridge, M., Elliott, R.N., Vaidyanathan, S., Laitner, S., Talbot, J., Trombley, D., Chittum, A., Black, S., Osann, E., Violette, D., Hagenstad, M., Schare, S., Darrow, K., Hampson, A., Hedman, B., White, D., Hornby, R., 2010. North Carolina's Energy Future: Electricity, Water, and Transportation Efficiency. Washington, D.C.
Fares, A., Fares, S., 2012. Irrigation management system, IMANSYS, a user-friendly computer based water management software package. In: Proceedings of the Irrigation Show and Education Conference. Orlanda, FL.
Fares, A., Awal, R., Fares, S., Johnson, A.B., Valenzuela, H., 2016. Irrigation water requirements for seed corn and coffee under potential climate change scenarios. J. Water Clim. Change 7, 39–51. https://doi.org/10.2166/wcc.2015.025.
Fares, A., Bayabil, H.K., Zekri, M., Mattos, D., Awal, R., 2017. Potential climate change impacts on citrus water requirement across major producing areas in the world. J. Water Clim. Change 8, 576–592. https://doi.org/10.2166/wcc.2017.182.
Field, C.B., Barros, V., Stocker, T.F., Dahe, Q., Dokken, D.J., Ebi, K.L., Mastrandrea, M.D., Mach, K.J., Plattner, G., Allen, S.K., Tignor, M., Midgley, P.M. (Eds.), 2012. Managing the Risks of Extreme Events and Disasters to Advance Climate Change Adaptation, A Special Report of Working Groups I and II of the Intergovernmental Panel on Climate Change. Cambridge University Press, New York, NY. https://doi.org/10.1017/cbo9781139177245.
Global Weather Data for SWAT, 2012 [WWW Document], URL. http://globalweather.tamu.edu/, 8.9.20.
Gosling, S.N., Arnell, N.W., 2016. A global assessment of the impact of climate change on water scarcity. Climatic Change 134, 371–385. https://doi.org/10.1007/s10584-013-0853-x.
Guo, R., Li, X., Christie, P., 2008. Influence of root zone nitrogen management and a summer catch crop on cucumber yield and soil mineral nitrogen dynamics in intensive production systems. Plant Soil 313, 55–70. https://doi.org/10.1007/s11104-008-9679-0.
Harrison, T., Winfree, R., 2015. Urban drivers of plant-pollinator interactions. Funct. Ecol. 29, 879–888. https://doi.org/10.1111/1365-2435.12486.
Hill, R.W., Barker, J.B., 2010. Verification of Turfgrass Evapotranspiration in Utah. Logan, UT.
Hodgson, K., Campbell, M.C., Bailkey, M., 2011. Urban Agriculture: growing healthy, sustainable places. In: APA Planning Advisory Service Report Number 563. Chicago, IL.
Hong, E.M., Nam, W.H., Choi, J.Y., Pachepsky, Y.A., 2016. Projected irrigation requirements for upland crops using soil moisture model under climate change in South Korea. Agric. Water Manag. 165, 163–180. https://doi.org/10.1016/j.agwat.2015.12.003.
Huang, K., Li, X., Liu, X., Seto, K.C., 2019. Projecting global urban land expansion and heat island intensification through 2050. Environ. Res. Lett. 14, 114037. https://doi.org/10.1088/1748-9326/ab4b71.
Hutmacher, R.B., Steiner, J.J., Ayars, J.E., Mantel, A.B., Vail, S.S., 1990. Response of seed carrot to various water regimes. I. Vegetative growth and plant water relations. J. Am. Soc. Hortic. Sci. 115, 715–721. https://doi.org/10.21273/jashs.115.5.715.
Jia, X., Dukes, M.D., Jacobs, J.M., 2009. Bahiagrass crop coefficients from eddy correlation measurements in central Florida. Irrigat. Sci. 28, 5–15. https://doi.org/10.1007/s00271-009-0176-x.
Jiang, L., Deng, X., Seto, K.C., 2013. The impact of urban expansion on agricultural land use intensity in China. Land Use Pol. 35, 33–39. https://doi.org/10.1016/j.landusepol.2013.04.011.
Jones, M.R., Singels, A., Ruane, A.C., 2015. Simulated impacts of climate change on water use and yield of irrigated sugarcane in South Africa. Agric. Syst. 139, 260–270. https://doi.org/10.1016/j.agsy.2015.07.007.
Khan, A.G., Anwar-ul-Hassan, Iqbal, M., Ullah, E., 2015. Assessing the performance of different irrigation techniques to enhance the water use efficiency and yield of maize under deficit water supply. Soil Environ. 34, 166–179.
Khan, A.G., Imran, M., Khan, A.U.H., Fares, A., Šimůnek, J., Ul-Haq, T., Alsahli, A.A., Alyemeni, M.N., Ali, S., 2021. Performance of spring and summer-sown maize under different irrigation strategies in Pakistan. Sustainability 13, 1–13. https://doi.org/10.3390/su13052757.
Kiziloglu, F.M., Sahin, U., Kuslu, Y., Tunc, T., 2009. Determining water-yield relationship, water use efficiency, crop and pan coefficients for silage maize in a semiarid region. Irrigat. Sci. 27, 129–137. https://doi.org/10.1007/s00271-008-0127-y.
Kulak, M., Graves, A., Chatterton, J., 2013. Reducing greenhouse gas emissions with urban agriculture: a Life Cycle Assessment perspective. Landsc. Urban Plann. 111, 68–78. https://doi.org/10.1016/j.landurbplan.2012.11.007.
Lin, B.B., Philpott, S.M., Jha, S., 2015. The future of urban agriculture and biodiversity-ecosystem services: challenges and next steps. Basic Appl. Ecol. 16, 189–201. https://doi.org/10.1016/j.baae.2015.01.005.
Liu, W., Hong, Y., Khan, S.I., Huang, M., Vieux, B., Caliskan, S., Grout, T., 2010. Actual evapotranspiration estimation for different land use and land cover in urban regions using Landsat 5 data. J. Appl. Remote Sens. 4, 041873 https://doi.org/10.1117/1.3525566.
Lovell, S.T., 2010. Multifunctional urban agriculture for sustainable land use planning in the United States. Sustainability 2, 2499–2522. https://doi.org/10.3390/su2082499.
Lupia, F., Baiocchi, V., Lelo, K., Pulighe, G., 2017. Exploring rooftop rainwater harvesting potential for food production in urban areas. Agriculture (Switzerland) 7, 1–17. https://doi.org/10.3390/agriculture7060046.
Mainuddin, M., Kirby, M., Chowdhury, R.A.R., Shah-Newaz, S.M., 2015. Spatial and temporal variations of, and the impact of climate change on, the dry season crop irrigation requirements in Bangladesh. Irrigat. Sci. 33, 107–120. https://doi.org/10.1007/s00271-014-0451-3.
Mal, S., Singh, R.B., Huggel, C. (Eds.), 2008. Climate Change, Extreme Events and Disaster Risk Reduction, towards Sustainable Development Goals. Springer International Publishing, Cham, Switzerland.
Martellozzo, F., Ramankutty, N., Hall, R.J., Price, D.T., Purdy, B., Friedl, M.A., 2015. Urbanization and the loss of prime farmland: a case study in the Calgary–Edmonton corridor of Alberta. Reg. Environ. Change 15, 881–893. https://doi.org/10.1007/s10113-014-0658-0.
Martinez Hernandez, J.J., Bar-Yosef, B., Kaikafi, U., 1991. Effect of surface and subsurface drip fertigation on sweet corn rooting, uptake, dry matter production and yield. Irrigat. Sci. 12, 153–159. https://doi.org/10.1007/BF00192287.
McClintock, N., 2008. From industrial garden to food desert: unearthing the root structure of urban agriculture in Oakland, California. In: ISSI Fellows Working Papers.
Meenar, M., Hoover, B., 2012. Community food security via urban agriculture: understanding people, place, economy, and accessibility from a food justice perspective. Journal of Agriculture, Food Syst. Commun. Dev. 3, 143–160. https://doi.org/10.5304/jafscd.2012.031.013.
Meinshausen, M., Raper, S.C.B., Wigley, T.M.L., 2011. Emulating coupled atmosphere-ocean and carbon cycle models with a simpler model, MAGICC6 - Part 1: model description and calibration. Atmos. Chem. Phys. 11, 1417–1456. https://doi.org/10.5194/acp-11-1417-2011.
Mishra, V., 2002. Population growth and intensification of land use in India. Int. J. Popul. Geogr. 8, 365–383. https://doi.org/10.1002/ijpg.266.
Moglia, M., 2014. Urban agriculture and related water supply: explorations and discussion. Habitat Int. 42, 273–280. https://doi.org/10.1016/j.habitatint.2014.01.008.
Mohareb, E., Heller, M., Novak, P., Goldstein, B., Fonoll, X., Raskin, L., 2017. Considerations for reducing food system energy demand while scaling up urban agriculture. Environ. Res. Lett. 12 https://doi.org/10.1088/1748-9326/aa889b.
Mok, H.F., 2020. 2030 GREENHOUSE GAS REDUCTION STRATEGY. San Jose, CA.
Mok, H.F., Williamson, V.G., Grove, J.R., Burry, K., Barker, S.F., Hamilton, A.J., 2014. Strawberry fields forever? Urban agriculture in developed countries: a review. Agron. Sustain. Dev. 34, 21–43. https://doi.org/10.1007/s13593-013-0156-7.
Mougeot, L.J.A., 2006. Growing Better Cities: Urban Agriculture for Sustainable Development. International Development Research Centre, Ottawa, ON, Canada.
Murphy, J.A., Hendricks, M.G., Rieke, P.E., Smucker, A.J.M., Branham, B.E., 1994. Turfgrass root systems evaluated using the minirhizotron and video recording methods. Agron. J. 250, 247–250. https://doi.org/10.2134/agronj1994.00021962008600020007x.

Nation, United, 2018. World Urbanization Prospects 2018. Department of Economic and Social Affairs. World Population Prospects 2018.
Nemadodzi, L.E., Araya, H., Nkomo, M., Ngezimana, W., Mudau, N.F., 2017. Nitrogen, phosphorus, and potassium effects on the physiology and biomass yield of baby spinach (Spinacia oleracea L.). J. Plant Nutr. 40, 2033–2044. https://doi.org/10.1080/01904167.2017.1346121.
Nogeire-McRae, T., Ryan, E.P., Jablonski, B.B.R., Carolan, M., Arathi, H.S., Brown, C.S., Saki, H.H., McKeen, S., Lapansky, E., Schipanski, M.E., 2018. The role of urban agriculture in a secure, healthy, and sustainable food system. Bioscience 68, 748–759. https://doi.org/10.1093/biosci/biy071.
Pannkuk, T.R., White, R.H., Steinke, K., Aitkenhead-Peterson, J.A., Chalmers, D.R., Thomas, J.C., 2010. Landscape coefficients for single- and mixed-species landscapes. Hortscience 45, 1529–1533. https://doi.org/10.21273/hortsci.45.10.1529.
Peters, C.J., Bills, N.L., Lembo, A.J., Wilkins, J.L., Fick, G.W., 2009. Mapping potential foodsheds in New York State: a spatial model for evaluating the capacity to localize food production. Renew. Agric. Food Syst. 24, 72–84. https://doi.org/10.1017/S1742170508002457.
Pinnix, G.D., Miller, G.L., 2019. Crop coefficients for tall fescue and hybrid bermudagrass in the transition zone. Crop. Forage Turfgrass Manag. 5, 190013. https://doi.org/10.2134/cftm2019.02.0013.
Pratt, J.W., Gibbons, J.D., 1981. Kolmogorov-smirnov two-sample tests. In: Concepts of Nonparametric Theory. Springer-Verlag New York Inc., New York, NY, pp. 318–344.
Reddy, V.R., Reddy, B.S., 2007. Land alienation and local communities: case studies in Hyderabad- Secunderabad. Econ. Polit. Wkly. 42, 3233–3240.
Riediger, J., Breckling, B., Nuske, R.S., Schröder, W., 2014. Will climate change increase irrigation requirements in agriculture of Central Europe? A simulation study for Northern Germany. Environ. Sci. Eur. 26, 1–13. https://doi.org/10.1186/s12302-014-0018-1.
Romero, C.C., Dukes, M.D., 2016. Review of turfgrass evapotranspiration and crop coefficients. Trans. ASABE 59, 207–223. https://doi.org/10.13031/trans.59.11180.
Saadi, S., Todorovic, M., Tanasijevic, L., Pereira, L.S., Pizzigalli, C., Lionello, P., 2015. Climate change and Mediterranean agriculture: impacts on winter wheat and tomato crop evapotranspiration, irrigation requirements and yield. Agric. Water Manag. 147, 103–115. https://doi.org/10.1016/j.agwat.2014.05.008.
Schewe, J., Heinke, J., Gerten, D., Haddeland, I., Arnell, N.W., Clark, D.B., Dankers, R., Eisner, S., Fekete, B.M., Colón-González, F.J., Gosling, S.N., Kim, H., Liu, X., Masaki, Y., Portmann, F.T., Satoh, Y., Stacke, T., Tang, Q., Wada, Y., Wisser, D., Albrecht, T., Frieler, K., Piontek, F., Warszawski, L., Kabat, P., 2014. Multimodel assessment of water scarcity under climate change. Proc. Natl. Acad. Sci. U. S. A. 111, 3245–3250. https://doi.org/10.1073/pnas.1222460110.
Semananda, N.P.K., Ward, J.D., Myers, B.R., 2016. Evaluating the efficiency of wicking bed irrigation systems for small-scale urban agriculture. Horticulturae 2. https://doi.org/10.3390/horticulturae2040013.
Seto, K.C., Ramankutty, N., 2016. Hidden linkages between urbanization and food systems. Science 352, 943–945. https://doi.org/10.1126/science.aaf7439.
Seto, K.C., Güneralp, B., Hutyra, L.R., 2012. Global forecasts of urban expansion to 2030 and direct impacts on biodiversity and carbon pools. Proc. Natl. Acad. Sci. U. S. A. 109, 16083–16088. https://doi.org/10.1073/pnas.1211658109.
Siegner, A., Sowerwine, J., Acey, C., 2018. Does urban agriculture improve food security? Examining the nexus of food access and distribution of urban produced foods in the United States: a systematic review. Sustainability 10, 8–12. https://doi.org/10.3390/su10092988.
Smajstrla, A.G., Zazueta, F.S., 1988. Simulation of irrigation requirements of Florida agronomic crops. Soil Crop Sci. Soc. Florida Proc. 47, 78–82.
Sowby, R.B., 2018. New Techniques to Analyze Energy Use and Inform Sustainable Planning, Design, and Operation of Public Water Systems. University of Utah.
State Electricity Profiles, 2020 [WWW Document], URL. https://www.eia.gov/electricity/state/.
Stott, P., 2016. How climate change affects extreme weather events. Science 352, 1517–1518. https://doi.org/10.1126/science.aaf7271.
Tanasijevic, L., Todorovic, M., Pereira, L.S., Pizzigalli, C., Lionello, P., 2014. Impacts of climate change on olive crop evapotranspiration and irrigation requirements in the Mediterranean region. Agric. Water Manag. 144, 54–68. https://doi.org/10.1016/j.agwat.2014.05.019.
Turfgrass Crop Coefficients (Kc), 2021 [WWW Document]. https://ucanr.edu/sites/UrbanHort/Water_Use_of_Turfgrass_and_Landscape_Plant_Materials/Turfgrass_Crop_Coefficients_Kc/.
United Nations, 2019. World Population Prospects 2019. Department of Economic and Social Affairs. World Population Prospects 2019.
Ward, J.D., Ward, P.J., Saint, C.P., Mantzioris, E., 2014. The urban agriculture revolution: implications for water use in cities. Water: J. Australia Water Assoc. 41, 69–74.
Williams, M.M., Lindquist, J.L., 2007. Influence of planting date and weed interference on sweet corn growth and development. Agron. J. 99, 1066–1072. https://doi.org/10.2134/agronj2007.0009.
Wortman, S.E., Lovell, S.T., 2013. Environmental challenges threatening the growth of urban agriculture in the United States. J. Environ. Qual. 42, 1283–1294. https://doi.org/10.2134/jeq2013.01.0031.
Wu, L., 1985. Matching irrigation to turfgrass root depth. California Turfgass Culture 35, 1–2.
Yonkin, M., Clubine, K., O'Connor, K., 2008. Importance of energy efficiency to the water and wastewater sector. Clearwaters 12–13.